European Review for Medical and Pharmacological Sciences 2013; 17: 1669-1680

RNA interference suppression of A100A4 reduces the growth and metastatic phenotype of human renal cancer cells via NF-κB-dependent MMP-2 and bcl-2 pathway

X.-C. YANG, X. WANG, L. LUO, D.-H. DONG, Q.-C. YU, X.-S. WANG, K. ZHAO

Department of Urology Surgery, the Affiliated Hospital of Medical College, Qingdao University, Qingdao, China

Abstract. – BACKGROUND AND AIM: S100A4 is a well established marker and mediator of metastatic disease, but the exact mechanisms responsible for the metastasis promoting effects are less well defined. We tested a hypothesis that the S100A4 gene plays a role in the proliferation and invasiveness of human renal cancer cells (RCC) and may be associated with its metastatic spread.

MATERIALS AND METHODS: The small interference RNA vector pcDNA3.1-S100A4 siRNA was transfected in to the human renal cancer cell lines ACHN, Ketr-3, OS-RC-2, CaKi-2 and HTB-47, then treated with ABT-737 or BB94. Cell apoptosis and cell viability was detected by flow cytometry and MTT assay. Matrigel was used for cell motility and invasion assay. MMP-2, bcl-2 and S100A4 was detected by RT-PCR and western blot assay. NF-κB subunit p65 activity was detected by confocal microscopy assay. We then determine the effect S100A4 sliencing on tumor growth, lung metastasis development *in vivo*. Immunohistochemistry was used to detected the expression of S100A4, bcl-2, MMP-2, p65 and CD31.

RESULTS: S100A4 silencing in ACHN cells by RNA interference significantly inhibited NF-κB and NF-κB-mediated MMP-2 and bcl-2 activation and cellular migration, proliferation, and promoted apoptosis. Furthermore, re-expression of S100A4 in S100A4-siRNA-transfected ACHN cells by transient S100A4 cDNA transfection restored the NF-κB and NF-κB-mediated MMP-2 and bcl-2 activation and their high migratory and cellular proliferative ability. An inhibitor ABT-737 (the Bcl-2 antagonist targets Bcl-2) against Bcl-2 suppressed cellular proliferation and promoted apoptosis induced by S100A4 re-expression in S100A4-siRNA-transfected ACHN cells. A inhibitor BB94 against MMPs to neutralize MMP-2 protein suppressed cellular invasion and migration induced by S100A4 re-expression in S100A4-siRNA-transfected ACHN cells. In the prevention model, S100A4 silencing inhibited primary tumor growth by (tumor weight) (76 ± 8%) and (tumor volum) (78 ± 4%) respectively and promoted apoptosis and the formation of lung metastases was inhibited by 89% ($p < 0.01$). Microvascular density was reduced by 70% ($p < 0.01$). In addition, S100A4 sliencing inhibited the expression of S100A4 *in vivo*, followed by the NF-κB, MMP-2 and bcl-2 suppression.

CONCLUSIONS: We conclude that S100A4 plays a crucial role in proliferation and migratory/invasive processes in human RCC by a mechanism involving activation of NF-κB-bcl-2 and NF-κB-MMP-2 pathway.

Key Words:
Renal cancer, S100A4, NF-κB, MMP-2, bcl-2.

Introduction

S100A4, also known as mts1, p9Ka, FSP1, CAPL, calvasculin, pEL98, metastasin, 18A2, and 42A, was cloned in the 1980s and early 1990s from various cell systems1. The human S100A4 gene is located in a frequently rearranged gene cluster on chromosome 1q21 and is composed of four exons, of which the first two are noncoding[1]. The 101-amino acid protein has a molecular mass of approximately 11.5 kDa and is characterized by the presence of two Ca^{2+}-binding EF-hands. Upon Ca^{2+}-binding, S100A4 undergoes a conformational change, forming a hydrophobic pocket essential for the recognition of target proteins[2].

It has been demonstrated in a number of studies that the S100A4 gene product is involved in the promotion of metastasis, angiogenesis, cell motility and expression of matrix metalloproteinases[3-7], but the exact molecular mechanisms by which extracellular S100A4 exerts these ef-

Corresponding Author: Xinsheng Wang, MD; e-mail: qyfywang@163.com

fects are incompletely elucidated. Xie et al[8] has reported S100A4 is a critical mediator of invasion in endometrial cancer and is upregulated by the TGF-beta-1 signaling pathway. Zhang et al[9] has found S100A4 may control invasion and metastasis in esophageal squamous cell carcinoma cell lines at least in part through the regulation of MMP-2 and E-cadherin activity.

The heterodimeric transcription factor NF-κB is a central player in cancer development and progression. Schematically, NF-κB can be activated through either the classical or the alternative pathway. A recent study has demonstrated that extracellular S100A4 could activate the transcription factor NF-κB in a subset of human cancer cell lines[10].

It has reported S100A4 and NF-κB overexpression was signicantly related with apoptosis, angiogenesis pulmonary metastases in renal cell carcinoma[11-14], and significant relation was shown between the two genes. We suggested that S100A4-stimulated transcription of the downstream target genes was dependent on activation of the NF-κB pathway.

The aim of the present study was to characterize S100A4-induced signal transduction mechanisms and to identify S100A4 target genes. We demonstrate that S100A4 can modulate the migratory, invasive and proliferative behavior of RCC cells *in vitro* and *in vivo*. S100A4 modulates proliferative behavior of RCC cells by NF-κB-dependent bcl-2 regulation, and S100A4 modulates the migratory and invasive behavior of RCC cells by NF-κB-dependent MMP-2 regulation.

Materials and Methods

Cell Culture and Antibodies

The human renal cancer cell lines ACHN, Ketr-3, OS-RC-2, CaKi-2 and HTB-47 were obtained from the American Type Culture Collection. The cells were cultured in DMEM/F12 containing 10% fetal bovine serum (FBS) supplemented with penicillin (50 U/ml), streptomycin (50 μg/ml) and amphotericin B (0.125 μg/ml) in a humidified atmosphere of 95% air and 5% CO_2. The primary polyclonal Anti-S100A4 (1:100; Santa Cruz Biotechnology Inc., Santa Cruz, CA, USA), Anti-MMP-2 (1:100; BD Biosciences, San Jose, CA, USA) and mouse monoclonal anti-NF-κB p65 and Anti-bcl-2 antibody (1:50; Boehringer Mannheim, Germany).

Stable pcDNA3.1-S100A4 siRNA Transfection

ACHN cultures were transfected with the pcDNA3.1 empty vector or the stable small interference RNA vector pcDNA3.1-S100A4 siRNA (v2MM_83072) using Lipofectamine 2000 Invitrogen, Carlsbad, CA, USA) as described by the manufacturer. Briefly, stable transfectants (clones) were selected from colonies growing in plates from a 10-fold dilution series in medium prepared with 10 μg/ml of puromycin antibiotic (Sigma Aldrich Co., St Louis, MO, USA). Clones were subjected to a second round of 10-fold dilutions and replated in puromycin medium and a second colony selection performed to provide clean clones for further analysis.

pcDNA3.1-S100A4 cDNA Plasmid Construction and Transient Transfection

pET15b-S100A4 plasmid was procured from Biovector Science Lab, Inc (Houston, TX, USA), and S100A4-cDNA was isolated from pET15b-S100A4 by using Nco I and BamH I restriction endonuclease. The digested fragment was then ligated into PcDNA3.1 vector (Invitrogen, Carlsbad, CA, USA) previously digested with Nco I and BamH I and treated with calf intestinal alkaline phosphatase. The resulting construct was verified by direct sequencing. For transfection studies, stable PcDNA3.1-S100A4 siRNA transfected ACHN cells were plated at a density of 1×10^6 cells per well in six-well plates and incubated for 24 h in complete medium. The cells were then transfected with 4 μg of the S100A4 construct by using a Lipofectamine™ for 48h. For controls, the same amount of empty vector, pGEX4T1 vector (as positive control for transfection) was also transfected for 48h.

ABT-737 and BB94 Treatment

To study the effect of re-inhibition of MMP-2/bcl-2 on the invasion,proliferation and apoptosis property in ACHN cells *in vitro*, stable pSM2-S100A4 siRNA transfected ACHN cells were plated at a density of 1×10^6 cells per well in six-well plates and incubated for 24 h in complete medium. The cells were then transfected with 4 μg of the S100A4 cDNA by using a Lipofectamine™ for 48 h, during which 0.1 mmol/mL BB94 (a specific MMPs inhibitor) or 10 μM ABT-737 (the Bcl-2 antagonist targets Bcl-2) was added into the culture.

Western Blotting

ACHN cells in various groups were harvested by trypsinization, washed with phosphate buffered saline (PBS), and lysed overnight at –20°C in a lysis buffer containing 20 mM Tris (pH 7.5), 150 mM NaCl, 1 mM EDTA, 1 mM Methylene glycol tetraacetic acid (EGTA), 1% Triton X-100, 2.5 mM sodium pyrophosphate, 1 mM β-glycerolphosphate, 1 mM Na_3VO_4, 1 µg/ml leupeptin, and 1 mM phenylmethylsufonyl fluoride (PMSF). Debris was sedimented by centrifugation for 10 min at 14.000 × g, and the protein concentration of the supernatant was determined using a Bio-Rad protein detection assay kit (Hercules, CA, USA). Proteins in the total cell lysate (40 ug of protein) were separated on 10% SDS-PAGE and electrotransferred to a polyvinylidene difluoride membrane (Immobilon-P membrane; Millipore, Bedford, MA, USA). After the blot was blocked in a solution of 5% skimmed milk, 0.1% Tween 20 and PBS, membrane-bound proteins were probed with primary antibodies against S100A4, MMP-2, bcl-2 and NF-KBp65. The membrane was washed and then incubated with horseradish peroxidase (HRP)-conjugated secondary antibodies for 30 minutes. Antibody-bound protein bands were detected with enhanced chemiluminescence reagents (Amersham Pharmacia Biotech, Piscataway, NJ, USA) and photographed with Kodak X-Omat Blue autoradiography film (Perkin Elmer Life Sciences, Boston, MA, USA).

RT-PCR

Total RNA was isolated from the transfected cells using the Qiagen RNeasy kit (Qiagen, Inc., Valencia, CA, USA) according to the manufacturer s protocol, and OneStep RT-PCR kit (Qiagen) was used for detecting mRNA expression of S100A4, MMP-2 and NF-κBp65. First-strand cDNA was prepared using Omniscript and Sensiscript reverse transcriptases at 50°C for 30 min. PCR amplification was then carried out under the following conditions: 95°C for 15 min, followed by 32 cycles at 94°C for 1 min, at 58°C for 1 min, and at 72°C for 1 min. The final extension was completed at 72°C for 10 min. The primers used are shown below: S100A4-forward, 5-CAGATCCTGACTGCTGCCATGGCG-32; S100A4-reverse, 5-ACGTGTCTGAAGGAGCCATGGTGG-3; MMP-9-forward, 5-TACCACCTCGAACTTTGACAGCGA-3; MMP-2-reverse: 52 -GACAGCGGTACAGTTCATGAGCA-32; forward: 52-AGGTACGTCAGTCTTATCTGTC-32; NF-κBP65: forward: 3-AGCACAGATACCAAGACCC-5; reverse: 5-CCCACGCTGCTCTTCTATAGGAAC-3; bcl-2-reverse: 5-TCTAGACGGCAGGTGAGGTCCACC-32, forward: 5-CCACCCATGGCAAATTCCATCGCA-32 .

Confocal Microscopy of NF-κB Subunit p65 Activity

Confocal microscopy was performed as described previously. Briefly, the ACHN cells in various time point in different groups (2×10^6 cells) were fixed on coverslips. After treatment, they were incubated with rabbit antihuman p65 antibody for 30 minutes and then washed with PBS. The cells were mounted onto microscope slides using mounting medium containing DAPI (4; 6-diamidino-2-phenylindole).

Gelatin Zymography

Gelatin zymography was performed using a Gelatinzymo electrophoresis kit (Yagai Research Center, Yamagata, Japan) according to the manufacturerís protocol.

Cell Viability Assay Using MTT

Cell viability was analysed by MTT assay [3-(4,5-dimethylthiazol-2-yl)-2,5 diphenyl tetrazolium bromide]. Cells in various time point in different groups (2×10^4 cells/well/100 µl) were seeded in 96-well plates. The culture volume was 100 µl. Twenty-four hours later, 10 µl of MTT from a 5 mg/ml stock in PBS was added to each well of the culture plates and incubated for 90 min at 37°C. The culture medium was removed and the purple crystals formed were dissolved in 150 µl isopropanol containing 0.1 N hydrochloric acid. The absorbance was read at 570 nm with a background correction of 690 nm in a VERSAmax microplate reader (Selby Biolab, Australia).

Flow Cytometry

The apoptosis was assessed by the ApopNexin fluorescein isothiocyanate (FITC) apoptosis detection kit (Chemicon, Billerica, MA, USA). The cells in various time point in different groups were detected by ApopNexin FITC apoptosis detection kit and flow cytometry (FACScalibur, BD, Franklin Lakes, NJ, USA) and data analyzed by WinMDI 2.8 free software (BD, USA).

Cell Motility and Invasion Assay

For the cell motility assay, the upper chambers (8 µm pore size) of transwells (Costar, San

Diego, CA, USA) were coated with collagen at 4°C. To prepare for the invasion assay, Matrigel (0.5 µg; Collaborative Research Co., Bedford, MA, USA) was diluted with cold water and dried onto each filter overnight at room temperature. After washing with PBS the next day, ACHN cells in various groups in different time point were added to the upper chamber using serum-free Dulbeccoís modified eagle medium (DMEM)/bovine serum albumin, and lysophosphatidic acid (LPA) was added to the lower chamber as a chemoattractant for 36h. The chamber was incubated for 2 h at 37°C with 10% CO_2. The cells that attached to the bottom side of the membrane were stained and counted using crystal violet. Assays were done in triplicate and repeated several times.

In vivo Experimental Metastasis Assays

Female C57BL/6 mice at 4-6 weeks old were obtained from Qingdao Medical college, Qingdao University for tumor implantation. All animals were maintained in a sterile environment and cared for within the laboratory animal regulations of the Ministry of Science and Technology of the People's Republic of China (http://www.most.gov.cn/kytj/kytjzcwj/200411). Full details of the study approval by the Ethics Committee at the Affiliated Hospital of Medical College, Qingdao University. ACHN cells (1×10^6) stablely transfected with pSM2-S100A4 siRNA plasmid were injected into the tail vein of 6- to 8-wk-old mice (n=8). After 21 days, the mice were sacrificed, and the lungs were fixed in Bouinís solution. Lung tumors were then analyzed below: first, by obtaining a surface tumor count, and second, by assessing tumor area in histologic sections from multiple depths throughout the lungs.

In vivo Experimental Growth Assays

For *in vivo* studies, 6×10^6 ACHN cells (stablely transfected with pSM2-S100A4 siRNA) contained in 200 µl of serum-free RPMI-1640 medium (Roswell Park Memorial Institute ñ 1640 medium) were delivered to mice by subcutaneous (s.c.) injection in each flank (10^7 cells/rat). The experiments were terminated 21 days tumor growth was monitored thrice a week by calipers to calculate tumor volumes according to the formula [length × width^2]/2. Tumor weights were determined at the end of the study when mice were sacrificed. All experiments were repeated at least twice. Representative experiments are shown.

Microvessel Density

The tumor vasculature was stained with an antibody against CD31, and microvessel density (MVD) was determined by counting CD31-stained vessels of tumor slides by examining ìhotspotsî according to standard procedures as described previously. In brief, sections were blocked in PBS + 5% rabbit serum and incubated overnight with monoclonal rat anti-mouse CD31 (PECAM-1) IgG (BD PharMingen, San Jose, CA, USA). Subsequently, sections were incubated with Dako LSAB 2 peroxidase-conjugated streptavidin (biotinylated rabbit anti-rat IgG, mouse absorbed; Vector Laboratories Inc., Burlingame, CA, USA), developed with 3,32 -diaminobenzidine, and counterstained with methyl green (Dako, Carpinteria, CA, USA). Vessel density per 200 field was quantified from 6 to 8 fields per tumor section from the treatment and control groups and expressed as percentage per area (200 × field). Percentage per area was assessed using ProImage software.

Immunohistochemistry

Immunohistochemical studies were done on 4-µm-thick sections derived from zinc-fixed, paraffin wax-embeded tumor tissue blocks. These tumors were harvested at the end of the experiments (after 22 days). Sections were subsequently dewaxed, rehydrated, and had endogenous peroxidase activity quenched before specific immunohistochemical staining for Anti-S100A4, Anti-MMP-2, Anti-bcl-2, Anti-NF-kBp65 and Anti-ki-67.

Terminal Deoxynucleotidyl Transferase-Mediated dUTP Nick end labeling Assay

Terminal deoxynucleotidyl transferase-mediated dUTP nick end labeling staining were done as described previously[15]. Staining intensity and localization for terminal deoxynucleotidyl transferase-mediated dUTP nick end labeling was scored by two investigators independently.

Results

Expression S100A4 mRNA and Protein in Human Renal Cancer Cell Lines

S100A4 mRNA and protein was detected by RT-PCR and western blot method in five human renal cancer cell lines ACHN, Ketr-3, OS-RC-2, CaKi-2 and HTB-47. As shown in Figure 1, the most significant expression of S100A4 mRNA

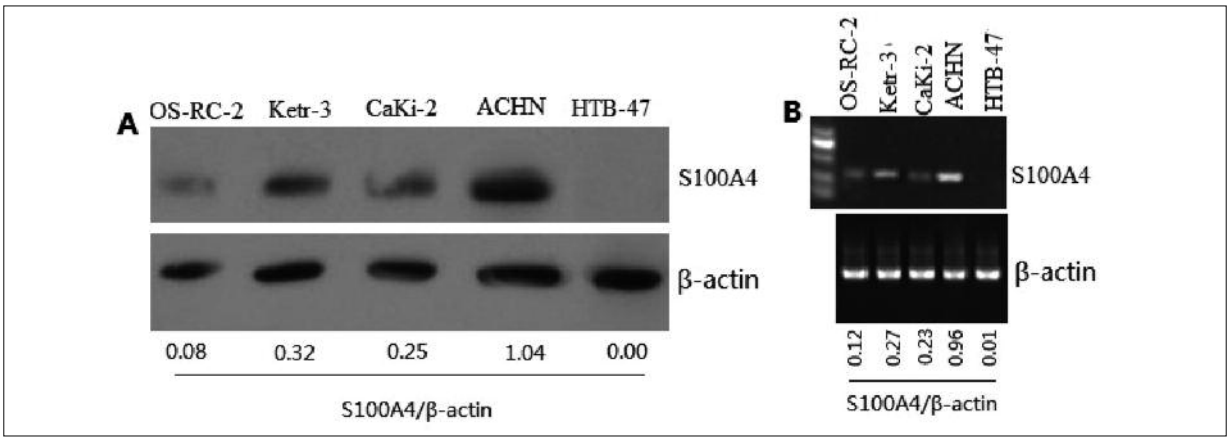

Figure 1. Expression S100A4 mRNA and protein in human renal cancer cell lines. ***A***, Western blot analysis; ***B,*** RT-PCR analysis. The most significant expression of the S100A4 mRNA and protein was shown in the ACHN cell line.

and protein was found in ACHN cell line. In the present study, ACHN cell line was used for further study.

Effect of siRNA on S100A4 Expression in ACHN Cells

As shown in Figure 2A, high (60-70%) transfection efficiency of siRNAs was observed in ACHN cells. As determined by Western blot analysis,cells stablely transfected with S100A4 siRNA completly inhibited the expression levels of S100A4 protein (Figure 2B). Nonsilencing siRNA (mock) did not exhibit any effect on protein levels of S100A4 (Figure 2B). Further, the suppression of S100A4 by siRNA in cells was confirmed by RT-PCR analysis. Cells transfected with S100A4 siRNA exhibited a significant reduction in mRNA level of S100A4 (Figure 2C). These data confirmed the suppression effect of siRNA and established the efficiency of siRNA transfection.

Effect of S100A4 Gene Knockdown on cell Survival and Apoptosis

To investigate the effect of S100A4 gene suppression on the growth of ACHN cells, we performed a MTT assay. As shown in Figure 2D, S100A4-siRNA-transfected ACHN cells showed a significantly reduced ($p < 0.01$) cell proliferative property compared with untreated and control siRNA-treated cells, suggesting that S100A4 might have growth-promoting effects on ACHN cells. To investigate the effect of S100A4 gene suppression on the apoptosis of ACHN cells, we performed a ApopNexin FITC apoptosis detection. As shown in Figure 2E, S100A4-siRNA-transfected ACHN cells showed a significantly increased ($p < 0.01$) cell apoptosis compared with untreated and control siRNA-treated cells, suggesting that S100A4 might have apoptosis-promoting effects on ACHN cells. We also found restoring the S100A4 in S100A4-siRNA-transfected ACHN cells could effectively inhibit the ACHN cell apoptosis and promote proliferative property (Figure 2 D and E).

Effect of S100A4 Gene Knockdown on cell Mobility and Invasion

Next, we analyzed the effect of S100A4 gene suppression on the invasive capability of highly invasive and metastatic ACHN cells by employing an *in vitro* chemoinvasion assay. As shown in Figure 2F, suppression of the S100A4 effectively blocks ACHN cell motility and invasion, and restoring the S100A4 in S100A4-siRNA-transfected ACHN cells could effectively promote the ACHN cell motility and invasion capability, suggesting that S100A4 is an essential component related to invasion ($p < 0.01$).

S100A4 Inhibition of the NF-κB-dependent bcl-2 Downregulation is Required for Cell Survival and Apoptosis

As shown in Figure 2 D and E, S100A4 inhibition could significantly promote cell apoptosis and suppress proliferative property, and vice versa. However, when the S100A4-siRNA-transfected ACHN cells were treated with ABT-737 combined with S100A4 cDNA, the proliferative property of ECA109 cells was inhibited and the apoptosis was promoted (Figure 2 D and E). We next analyzed whether the effect of S100A4

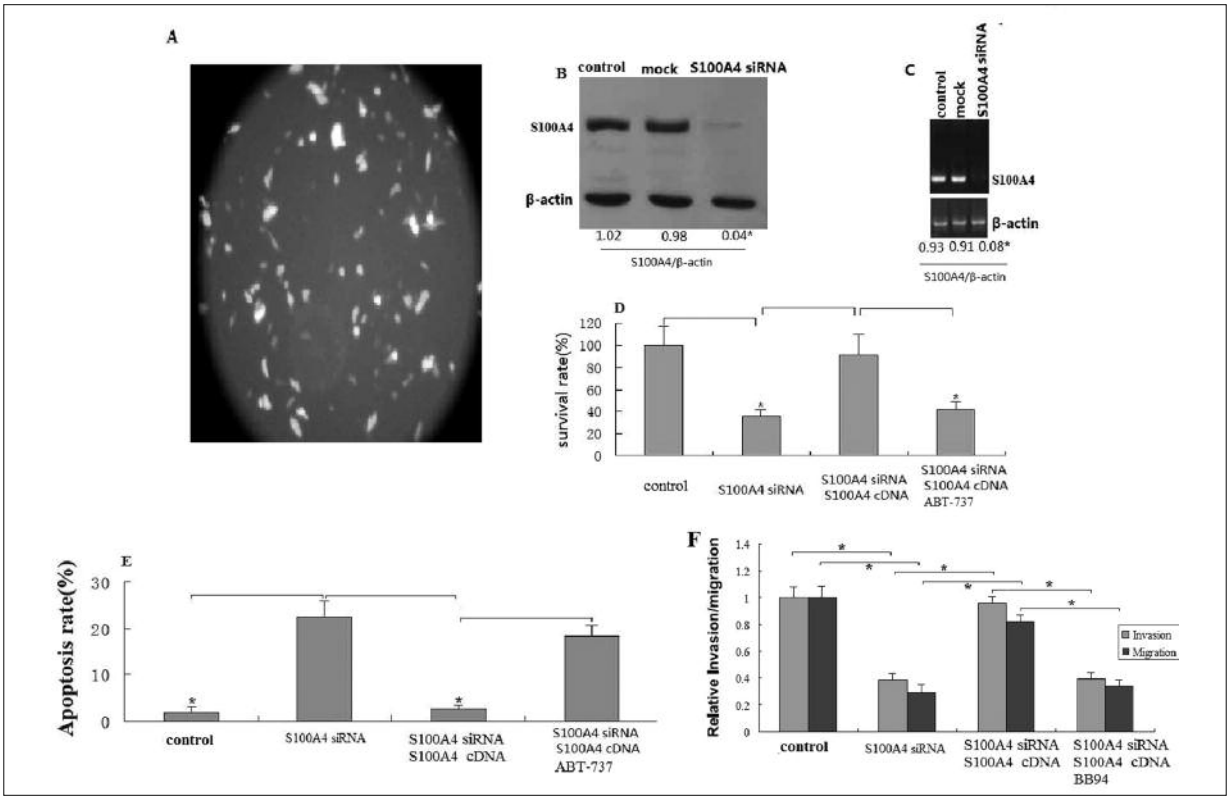

Figure 2. S100A4 gene knockdown by siRNA transfection in ACHN cells. ***A,*** Photomicrographs showing transfection of fluorescein-labeled siRNA in ACHN cells. ***B, C,*** Representative images showing expression of S100A4 protein and mRNA in nonsilencing siRNA control and S100A4-siRNA transfected cells as analyzed by Western (B) and RT-PCR (C). Equal loading of protein was confirmed by stripping the blots and reprobing with-actin antibody. Densitometric measurements of the bands in Western and RT-PCR analyses were performed by using the digitizing software UN-SCAN-IT (Silk Scientific, Orem, UT, USA). ***D,*** Photomicrographs showing survival cells and histogram showing the survival rate in untreated ACHN cells, pSM2-S100A4 siRNA transfected ACHN cells, transient transfection of pGEX4T-S100A4 cDNA in pSM2-S100A4 siRNA transfected ACHN cells. ***E,*** Flow cytometric analysis of PI-Annexin-V to quantify S100A4-induced apoptosis in untreated ACHN cells, pSM2-S100A4 siRNA transfected ACHN cells, transient transfection of pGEX4T-S100A4 cDNA in pSM2-S100A4 siRNA transfected ACHN cells. Each bar represents mean ± SE; $*p < 0.05$. All experiments were repeated three times with similar results. ***F,*** The ability of the cell lines mentioned to migrate or invade was measured using a transwell cell motility assay as described in the Materials and Methods section. Representative histogram showing invasive capability in pSM2-S100A4 siRNA transfected ACHN cells, transient transfection of pGEX4T-S100A4 cDNA in pSM2-S100A4 siRNA transfected ACHN cells or/and BB94 treatment. Each bar represents mean ± SE; the statistical analysis was done using the Student's I test. $p*< 0.01$ compared with the results of the controls. All experiments were repeated three times with similar results. These data suggest that the S100A4 gene controls the motility and invasion of ACHN cells through NF-κB/MMP-2 pathway.

inhibition on survival and apoptosis was by NF-κB-dependent bcl-2 activity. NF-κB subunit p65 activity was detected by confocal Microscopy (Figure 3A), bcl-2 mRNA (Figure 3 G) and p65 mRNA (Figure 3 C) and protein (Figure 3 B and H) was detected by western blot and RT-PCR. It was showed S100A4-siRNA-transfected ACHN cells showed a significantly decreased bcl-2 mRNA, p65 mRNA and protein expression. When the S100A4 siRNA transfected ACHN cells were re-expressed the S100A4 through transient S100A4 cDNA transfection for 48h, bcl-2 mRNA, p65 mRNA and protein expression was significantly induced (Figure 3A-C). However, when the S100A4-siRNA-transfected ACHN cells were treated with ABT-737 combined with S100A4 cDNA, bcl-2 protein was significantly inhibited (Figure 3 H), suggesting that S100A4-dependent NF-κB-bcl-2 is an essential component related to proliferation.

S100A4 Inhibition of the NF-κB-dependent MMP-2 Downregulation is Required for Cell Invasion

As shown in Figure 2 F, S100A4 inhibition could significantly suppress invasion and motility

in ACHN cells, and vice versa. We next analyzed whether the effect of S100A4 inhibition on invasion and motility was by NF-κB-dependent MMP-2 regulation. MMP-2 activity was detected by gelatin zymography (Figure 3D), MMP-2 mRNA and protein was detected by western blot (Figure 3 E) and RT-PCR (Figure 3F). It was showed S100A4-siRNA-transfected ACHN cells showed a significantly decreased MMP-2 mRNA and protein expression. When the S100A4 siRNA

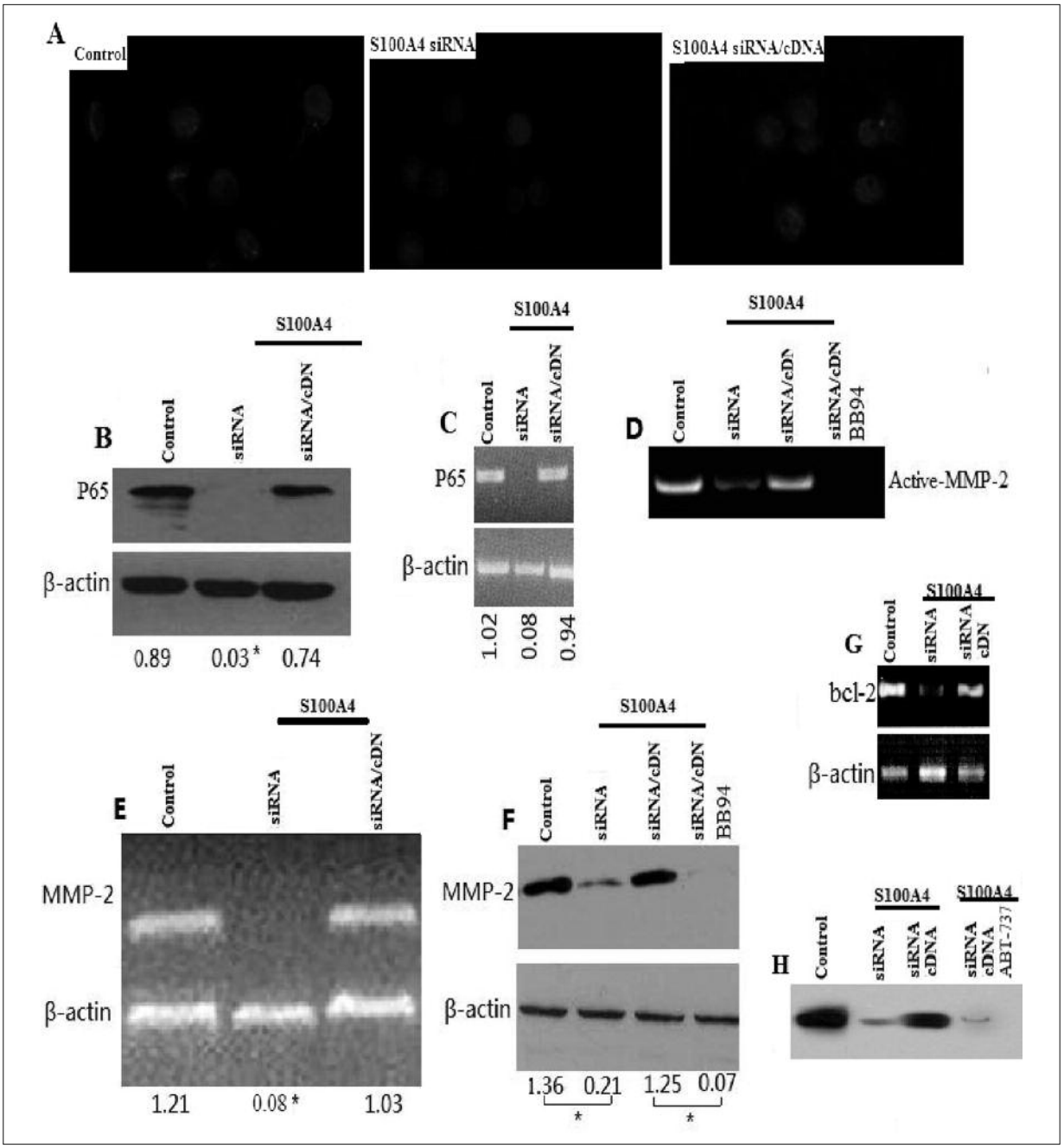

Figure 3. Diminished NF-κB activity in S100A4 siRNA-treated ACHN cells. ***A,*** ACHN cells were examined for their NF-κB activity by confocal microscopy of NF-κB subunit p50/65 localization. The ACHN cells were stained for p50/65 (red). DAPI (blue) indicates nucleus, where active form of NF-κB subunit p50/65 is found. ***B,*** Western blot analysis for P65. ***C,*** RT-PCR analysis for P65. ***D,*** Representative image showing gelatinolytic activity of MMP-2 in transfected cells. ***E,*** RT-PCR analysis for MMP-2. F, Western blot analysis for MMP-2. Each value represents mean ± SE; $*p < 0.01$. All experiments were repeated three times with similar results.

transfected ACHN cells were re-expressed the S100A4 through transient S100A4 cDNA transfection for 48h, MMP-2 mRNA and protein was significantly induced (Figure 3 D-F). Although S100A4 overexpression in S100A4 siRNA transfected ACHN cells restored the invasive ability (Figure 2F), followed by the NF-κB and MMP-2 upregulation (Figure 3 D-F), treatment with BB94 to inhibit MMP-2 activity significantly inhibited the invasion ability in the S100A4 cDNA transfected ACHN cells (Figure 2F).

Knockdown of S100A4 Inhibits ACHN Tumor Growth

To determine the effect S100A4 sliencing on tumor development *in vivo*, stablely transfected with pSM2-S100A4 siRNA contained in 200 μl of serum-free RPMI-1640 medium were delivered to mice by subcutaneous (s.c.) injection in each flank (107 cells/rat). Treatment with pSM2-S100A4 siRNA inhibited primary tumor growth by (tumor weight) 76 ± 8% (Figure 4 A; n = 8; $p < 0.001$) and (tumor volume) 78 ± 4% (Figure 4 B; n = 8; $p = 0.002$), respectively. No significant changes in weight and volume of the mock treated animals were observed during treatment compared to controls. Figure 4 C also shows that knockdown of S100A4 induced significantly tumor cell apoptosis as measured by TUNEL staining. To determine whether the significant inhibitory activity of S100A4-silencing on ACHN tumor growth *in vivo* was due in part to a downregulation of NF-κB, bcl-2 and MMP-2, immunohistochemistry staining was done to detect the expression of S100A4, NF-Kb, bcl-2, Anti-ki-67and MMP-2 in the tumor of the flank. The results shown reduced expression of S100A4 was found in S100A4 siRNA groups, followed by the downregulation of Ki-67 (Figure 4 D) and NF-κB, bcl-2 and MMP-2 (data not shown).

Knockdown of S100A4 Inhibits ACHN cells Lung Metastasis

Significantly decreased tumor nodes in S100A4 siRNA transfected groups were found. In S100A4 siRNA transfected groups, lack of S100A4 had a significant effect on development of lung metastasis in surface tumor number (Figure 5A). To further examine the metastatic lesions, we sectioned the lungs to obtain represen-

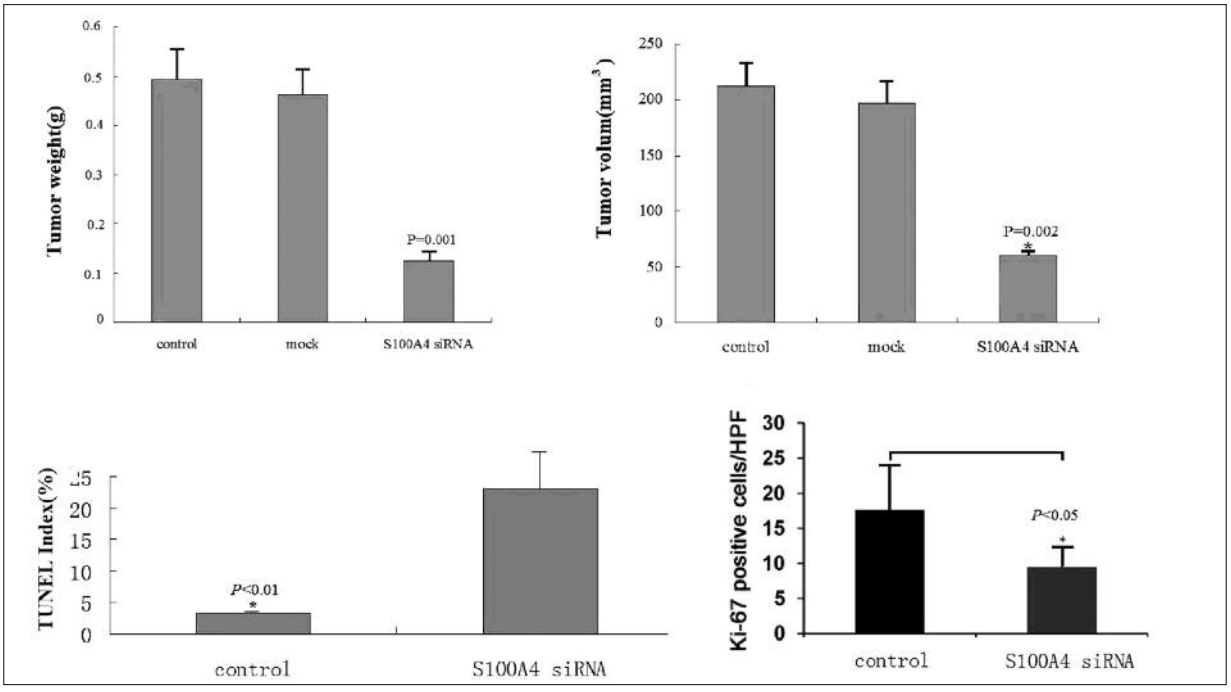

Figure 4. *In vivo* antitumor activity of S100A4 siRNA against s.c. xenografted tumors of ACHN cells in mice. ***A,*** Tumor weights were determined at the end of the study when mice were sacrificed. A significant reduction in tumor weigh was observed in a S100A4 siRNA groups 21 days after the start of treatment ($p = 0.001$). ***B,*** Tumor were determined at the end of the study when mice were sacrificed. A significant reduction in tumor weigh was observed in a S100A4 siRNA groups 21 days after the start of treatment ($p = 0.002$). ***C,*** TUNEL staining in the tumors, significantly increased apoptosis index was shown in S100A4 siRNA groups ($p < 0.01$). ***D,*** Low Ki-67 expression was shown in S100A4 siRNA groups ($p < 0.05$).

tative tissue from multiple depths. These were then assessed morphometrically to determine the percent area of lung parenchyma occupied by tumor lesions. Similarly to the gross surface counts, we observed a significant reduction in tumor burden in the lungs of S100A4 siRNA transfected mice compared with the littermate controls (Figure 5 B). To determine whether S100A4 blockade has an effect on ACHN tumor vasculature, MVD was analyzed. New blood vessel formation was significantly reduced in S100A4 siRNA transfected ACHN tumor. The vasculature in S100A4 siRNA-treated tumors was (0.38 ± 0.16%) versus 1.24 ± 0.19% in controls (Figure 5 C; $p < 0.01$).

Discussion

Metastasis is generally defined as the spread of malignant cells from the primary tumor through the circulation to establish secondary growth in a distant organ. Studies in rodents have provided evidence supporting the direct involvement of S100A4 in tumor progression and metastasis. The results of the present study show that S100A4 silencing suppressed the proliferation, invasion and promoted apoptosis of renal cancer cells *in vitro*, inhibited xenograft tumour formation, angiogenesis, and lung metastasis *in vivo*, and S100A4 inactivation was necessary for the growth and metastasis inhibition of experimental tumours *in vivo*. Although the S100A4 gene product is involved in the promotion of metastasis, angiogenesis, cell motility of renal cancer, but the exact molecular mechanisms by which extracellular S100A4 exerts these effects are incompletely elucidated.

The NF-κB signal transduction pathway is misregulated in a variety of hematologic and solid tumor malignancies due either to genetic changes, such as chromosomal rearrangements, amplifications, and mutations, or to chronic activation of the pathway. Constitutive activation of the NF-κB pathway can contribute to the oncogenic state by driving proliferation,enhancing cell survival, and/or promoting angiogenesis or metastasis[16]. As shown previously, NF-κB was activated in renal cell carcinoma[17], and targeting the nuclear factor-kB pathway could efficiently suppress proliferation and angiogenesis or metastasis[18-20].

In this study, we demonstrate that the molecular mechanism by which S100A4-confers cellular metastatic and proliferative ability is mediated by NF-κB activity and subsequent MMP-2 and bcl-2 upregulation. This is based on the following evidence. First, S100A4 silencing appreciably decreases the migratory and proliferative ability, and promotes apoptosis of ACHN cells. Conversely, restoring of S100A4 in S100A4 siRNA transfected ACHN cells increases the migratory and proliferative ability. Second, S100A4 silencing inhibits the NF-κB activity, followed by the downregulation of bcl-2 and MMP-2, and vice versa. Third, NF-κB-dependent bcl-2 activation is essential for the S100A4-mediated proliferative effects. Fourth, NF-κB-dependent MMP-2 activation is essential for the S100A4-mediated cellular metastatic effects. Finally, the NF-κB is regulated by prometastatic S100A4 gene and contributes to the metastatic and proliferative ability.

We presently found that S100A4 induces cell migration and promotes proliferation in an NF-KB-dependent manner. Thus, NF-KB signaling, which is vital for RCC cell migration and proliferation, is regulated by S100A4 and contributes to the increased migratory and proliferative ability. Activated NF-κB regulates migratory and proliferative ability via various substrates.

NF-κB transcription factors can regulate the expression of over 100 different genes dependent on the various functional forms of NF-κB, the stimulus of NF-κB activation and cell type examined. NF-κkB has been shown to regulate transcriptionally the expression of several members of the BCL-2 gene family, including bcl-2 antiapoptotic protein19. In our study, knockdown of S100A4 suppressed the NF-κB activity, followed by decreased proliferative ability in ACHN cells, and vice versa. We therefore suggested that S100A4 regulates proliferative ability of ACHN cells via NF-κB-dependent pathway. Furthermore, bcl-2 was regulated by S100A4-dependent NF-κB activity, and neutralizing of bcl-2 by ABT-737, a specific bcl-2 inhibitor, inhibits proliferative ability of ACHN cells though NF-κB was activated. We concluded S100A4 promots proliferative ability of ACHN cells via NF-κB-bcl-2 pathway.

Matrix metalloproteinases (MMPs) play an essential role in migration and invasion, and several experimental strategies have established an intimate connection between S100A4 and certain members of the MMP family[20-23]. Down-regulation of S100A4 expression in osteosarcoma cells led to reduced expression of MMP-2 and MT1-

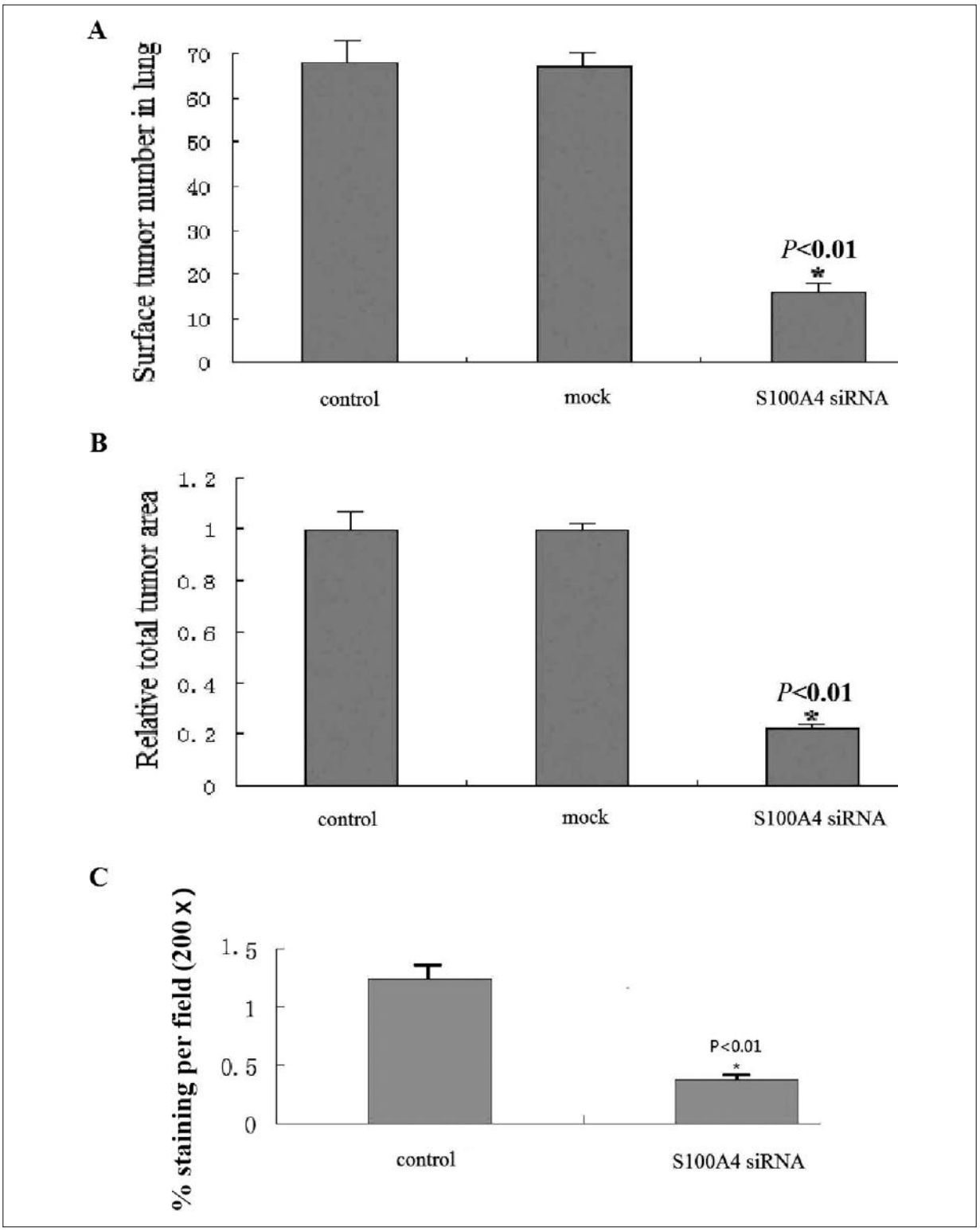

Figure 5. The effect of S100A4 siRNA inhibits ACHN cells lung metastasis. ***A,*** Representative histogram showing the surface tumor number in S100A4 siRNA groups. ***B,*** Representative histogram showing the total tumor area in the lungs in S100A4 siRNA groups. ***C,*** Representative area of the vascular density of the tumor from control versus S100A4 siRNA-treated mice. Quantification of the red staining revealed that the percentage area occupied by vasculature in S100A4 siRNA-treated tumors was 0.38 ± 0.16% versus 1.24 ± 0.19 % in controls $*p < 0.01$. Each bar represents mean ± SE; All experiments were repeated three times with similar results.

MMP, with a subsequent reduction in MMP-2 activity and a reduced ability to migrate through Matrigel-coated filters[24]. Based on observations in transgenic mice, S100A4 has been identified as a potent stimulator of angiogenesis. Augmented MMP-13 expression in endothelial cells was associated with S100A4-mediated stimulation of capillary-like growth in three-dimensional Matrigel cultures in vitro[23] and through interaction with annexin II, extracellular S100A4 accelerated tissue plasminogen activator-mediated conversion of plasminogen to plasmin, resulting in capillary-like tube formation of human cerebromicrovascular endothelial cells[25]. Interestingly, S100A4-stimulated plasmin activation may also contribute to the observed activation of MMP-2 and MMP-13. But the mechanisms by which S100A4 participates in the regulation of MMPs are mostly unknown. In this study, knockdown of S100A4 suppressed the NF-κB activity, followed by the decreased migratory and invasive ability in ACHN cells, and vice versa. We, therefore, suggested that S100A4 regulates migratory and invasive ability of ACHN cells via NF-κB-dependent pathway. In addition, MMP-2 was regulated by S100A4-dependent NF-κB activity, and neutralizing of MMP-2 by BB94, a specific MMPs inhibitor, inhibits migratory and invasive ability of ACHN cells though NF-κB was activated. We concluded S100A4 promots migratory and invasive ability of ACHN cells via NF-κB-MMP-2 pathway.

In our study, we further investigated the effect of S100A4 silencing on ACHN cells *in vivo*. The results indicated S100A4 silencing is a very potent way against an aggressive orthotopically implanted kidney tumor in mice. S100A4 silencing significantly inhibits primary tumor growth, angiogenesis and lung metastasis formation, and promotes apoptosis in this murine model.

Conclusions

We provide a detailed mechanism describing the potential role of S100A4 in migratory, angiogenesis, metastasis and proliferative ability behavior via a NF-κB-dependent upregulation of bcl-2 and MMP-2. This is the first identification of a new molecular mechanism of S100A4-driven prometastatic and proliferative pathway, possibly providing a new target for therapeutic intervention in metastatic RCC.

References

1) Garrett SC, Varney KM, Weber DJ, Bresnick AR. S100A4, a mediator of metastasis. J Biol Chem 2006; 281: 677-680.
2) Malashkevich VN, Varney KM, Garrett SC, Wilder PT, Knight D, Charpentier TH, Ramagopal UA, Almo SC, Weber DJ, Bresnick AR. Structure of Ca2+-bound S100A4 and its interaction with peptides derived from nonmuscle myosin-IIA. Biochemistry 2008; 47: 5111-5126.
3) Schmidt-Hansen B, Ornas D, Grigorian M, Klingelhofer J, Tulchinsky E, Lukanidin E, Ambartsumian N. Extracellular S100A4 (mts1) stimulates invasive growth of mouse endothelial cells and modulates MMP-13 matrix metalloproteinase activity. Oncogene 2004; 23: 5487-5495.
4) Belot N, Pochet R, Heizmann CW, Kiss R, Decaestecker C. Extracellular S100A4 stimulates the migration rate of astrocytic tumor cells by modifying the organization of their actin cytoskeleton. Biochim Biophys Acta 2002; 1600: 74-83.
5) Semov A, Moreno MJ, Onichtchenko A, Abulrob A, Ball M, Ekiel I, Pietrzynski G, Stanimirovic D, Alakhov V. Metastasis-associated protein S100A4 induces angiogenesis through interaction with Annexin II and accelerated plasmin formation. J Biol Chem 2005; 280: 20833-20841.
6) Schmidt-Hansen B, Klingelhofer J, Grum-Schwensen B, Christensen A, Andresen S, Kruse C, Hansen T, Ambartsumian N, Lukanidin E, Grigorian M. Functional significance of metastasis-inducing S100A4 (Mts1) in tumor-stroma interplay. J Biol Chem 2004; 279: 24498-24504.
7) Yammani RR, Carlson CS, Bresnick AR, Loeser RF. Increase in production of matrix metalloproteinase 13 by human articular chondrocytes due to stimulation with S100A4: role of the receptor for advanced glycation end products. Arthritis Rheum 2006; 54: 2901-2911.
8) Xie R, Schlumbrecht MP, Shipley GL, Xie S, Bassett RL Jr, Broaddus RR. S100A4 mediates endometrial cancer invasion and is a target of TGF-beta1 signaling. Lab Invest 2009; 89: 937-947.
9) Zhang HY, Zheng XZ, Wang XH, Xuan XY, Wang F, Li SS. S100A4 mediated cell invasion and metastasis of esophageal squamous cell carcinoma via the regulation of MMP-2 and E-cadherin activity. Mol Biol Rep 2012; 39: 199-208.
10) Grotterød I, Maelandsmo GM, Boye K. Signal transduction mechanisms involved in S100A4-induced activation of the transcription factor NF-kappaB. BMC Cancer 2010; 10: 241.
11) Bandiera A, Melloni G, Freschi M, Giovanardi M, Carretta A, Borri A, Ciriaco P, Zannini P. Prognostic factors and analysis of S100A4 protein in resected pulmonary metastases from renal cell carcinoma. World J Surg 2009; 33: 1414-1420.
12) Meteoglu I, Erdogdu IH, Meydan N, Erkus M, Barutca S. NF-KappaB expression correlates with

apoptosis and angiogenesis in clear cell renal cell carcinoma tissues. J Exp Clin Cancer Res 2008; 27: 53.

13) Sourbier C, Danilin S, Lindner V, Steger J, Rothhut S, Meyer N, Jacqmin D, Helwig JJ, Lang H, Massfelder T. Targeting the nuclear factor-kappaB rescue pathway has promising future in human renal cell carcinoma therapy. Cancer Res 2007; 67: 11668-11676.

14) Oya M, Takayanagi A, Horiguchi A, Mizuno R, Ohtsubo M, Marumo K, Shimizu N, Murai M. Increased nuclear factor-kappa B activation is related to the tumor development of renal cell carcinoma. Carcinogenesis 2003; 24: 377-384.

15) Jiao X, Liu X, Zhang B, Wang J, Wang Q, Tao Y, Zhang D. Knockdown of snail sensitizes pancreatic cancer cells to chemotherapeutic agents and irradiation. Int J Mol Sci 2010; 11: 4891-4892.

16) Wan F, Lenardo MJ. The nuclear signaling of NF-kappaB: current knowledge, new insights, and future perspectives. Cell Res 2010; 20: 24-33.

17) Oya M, Takayanagi A, Horiguchi A, Mizuno R, Ohtsubo M, Marumo K, Shimizu N, Murai M. Increased nuclear factor-kappa B activation is related to the tumor development of renal cell carcinoma. Carcinogenesis 2003; 24: 377-384.

18) Sourbier C, Danilin S, Lindner V, Steger J, Rothhut S, Meyer N, Jacqmin D, Helwig JJ, Lang H, Massfelder T. Targeting the nuclear factor-kappaB rescue pathway has promising future in human renal cell carcinoma therapy. Cancer Res 2007; 67: 11668-11676.

19) Morais C, Healy H, Johnson DW, Gobe G. Inhibition of nuclear factor kappa B attenuates tumour progression in an animal model of renal cell carcinoma. Nephrol Dial Transplant 2010; 25: 1462-1474.

20) Sourbier C, Danilin S, Lindner V. Targeting the nuclear factor-kb rescue pathway has promising future in human renal cell carcinoma therapy. Cancer Res 2007; 67: 11668-11676.

21) Kikuchi N, Horiuchi A, Osada R, Imai T, Wang C, Chen X, Konishi I. Nuclear expression of S100A4 is associated with aggressive behavior of epithelial ovarian carcinoma: an important autocrine/paracrine factor in tumor progression. Cancer Sci 2006; 97: 1061-1069.

22) Schmidt-Hansen B, Klingelhofer J, Grum-Schwensen B, Christensen A, Andresen S, Kruse C, Hansen T, Ambartsumian N, Lukanidin E, Grigorian M. Functional significance of metastasis-inducing S100A4 (Mts1) intumor-stroma interplay. J Biol Chem 2004; 279: 24498-24504.

23) Yammani RR, Carlson CS, Bresnick AR, Loeser RF. Increase in production of matrix metalloproteinase 13 by human articular chondrocytes due to stimulation with S100A4: role of the receptor for advanced glycation end products. Arthritis Rheum 2006; 54: 2901-2911.

24) Schmidt-Hansen B, Ornas D, Grigorian M, Klingelhofer J, Tulchinsky E, Lukanidin E, Ambartsumian N. Extracellular S100A4 (mts1) stimulates invasive growth of mouse endothelial cells and modulates MMP-13 matrix metalloproteinase activity. Oncogene 2004; 23: 5487-5495.

25) Bjørnland K, Winberg JO, Odegaard OT, Hovig E, Loennechen T, Aasen AO, Fodstad O, Maelandsmo GM. S100A4 involvement in metastasis: deregulation of matrix metalloproteinases and tissue inhibitors of matrix metalloproteinases in osteosarcoma cells transfected with an anti-S100A4 ribozyme. Cancer Res 1999; 59: 4702-4708.

26) Semov A, Moreno MJ, Onichtchenko A, Abulrob A, Ball M, Ekiel I, Pietrzynski G, Stanimirovic D, Alakhov V. Metastasis-associated protein S100A4 induces angiogenesis through interaction with Annexin II and accelerated plasmin formation. J Biol Chem 2005; 280: 20833-20841.